

# Cation Distribution and Stress Sensitivity of Cobalt Ferrite

Kakade SG<sup>1\*</sup>, kambale RC<sup>2</sup>, Mathe VL<sup>3</sup> and Kolekar YD<sup>4</sup>

<sup>1</sup>Department of Physics, Sir Parashurambhau College, Pune, Maharashtra, India-411 030,

<sup>2</sup>Department of Physics, Savitribai Phule Pune University, Pune, Maharashtra, India-411 007

Email: [sundipkakade@gmail.com](mailto:sundipkakade@gmail.com)

## Manuscript Details

Available online on <http://www.irjse.in>

ISSN: 2322-0015

Editor: Dr. Arvind Chavhan

## Cite this article as:

Kakade SG, kambale RC, Mathe VL and Kolekar YD. Cation Distribution and Stress Sensitivity of Cobalt Ferrite, *Int. Res. Journal of Science & Engineering*, January 2018; Special Issue A2 :156-160.

© The Author(s). 2018 Open Access

This article is distributed under the terms of the Creative Commons Attribution

4.0 International License

(<http://creativecommons.org/licenses/by/4.0/>),

which permits unrestricted use, distribution, and reproduction in any medium, provided you give appropriate credit to the original author(s) and the source, provide a link to the Creative Commons license, and indicate if changes were made.

## ABSTRACT

Cobalt ferrite (CoFe<sub>2</sub>O<sub>4</sub>) nanoparticles were synthesized by sol-gel auto combustion method. The pure spinel phase formation of face centered cubic lattice was confirmed using X-ray diffraction technique. We have investigated the structural, cation distribution using Mössbauer spectroscopy and magnetostrictive properties of synthesized cobalt ferrite nanoparticles. FE-SEM image show the almost spherical nanoparticles of cobalt ferrite (CFO) with the particle size of 42 nm. The presence of two vibrational bands in IR spectrum around 694 cm<sup>-1</sup> ( $\nu_1$ ) and 458 cm<sup>-1</sup> ( $\nu_2$ ) are associated with the tetrahedral and octahedral group complexes of the spinel lattice. The synthesized cobalt ferrite at nanoscale shows the maximum values of the magnetostrictive coefficient ( $\lambda_{11} = -240$  ppm and  $\lambda_{12} = 122$  ppm) at the lower value of applied magnetic field (6 kOe). Mössbauer spectroscopy shows that the cobalt ferrite at nanodimension is not perfectly spinel. The cobalt ferrites nanoparticles should be the promising candidates for automotive stress sensing.

**Keywords:** Cobalt ferrite, I-R Spectroscopy, FE-SEM, Cation Distribution, Stress Sensitivity

## INTRODUCTION

Magnetic oxide nanoparticles attract increasing interest in fundamental sciences as well as in technological applications. Ferrite is a generic term for a class of magnetic iron oxide compounds. Cobalt ferrite ( $\text{CoFe}_2\text{O}_4$ ) exhibits unique properties like strong spin-orbit coupling, high coercivity, high magneto-crystalline anisotropy, high Curie temperature and spontaneous magnetization [1–3].  $\text{CoFe}_2\text{O}_4$  (CFO) is utilized in the development of microwave devices, solar cells, spintronics, transducers and actuators [1–3]. Various ferrites and natural magnetite were used for actinide and heavy metal removal from wastewater [4]. Also, the most chemotherapeutic approaches to cancer treatments are non-specific in nature. Moreover, the targeted delivery of anti-tumor agents adsorbed on the surface of MNPs is a promising alternative to the conventional chemotherapy [5]. In consideration of the different applications of cobalt ferrite in magnetostrictive sensing, we have synthesized cobalt ferrite particles in nanometer regime. The application of synthesized CFO nanoparticles depends upon the site occupancy of metal cation among spinel structure, therefore, it is important to obtain the distribution of cations among spinel structure [2-3, 6]. Mössbauer spectroscopy is mostly utilized and most accurate technique to determine site occupancy [3,6].

## METHODOLOGY

### Synthesis:

The nanoparticles of Cobalt ferrite ( $\text{CoFe}_2\text{O}_4$ ) have been synthesized by sol gel autocombustion method. The analytical grade raw materials,  $\text{Co}(\text{NO}_3)_2 \cdot 6\text{H}_2\text{O}$ ,  $\text{Fe}(\text{NO}_3)_3 \cdot 9\text{H}_2\text{O}$ ,  $\text{C}_6\text{H}_8\text{O}_7 \cdot \text{H}_2\text{O}$  and  $\text{NH}_3 \cdot \text{H}_2\text{O}$  were utilized for the synthesis of CFO. Initially,  $\text{Co}(\text{NO}_3)_2 \cdot 6\text{H}_2\text{O}$  and  $\text{Fe}(\text{NO}_3)_3 \cdot 9\text{H}_2\text{O}$  were dissolved in the  $\text{C}_6\text{H}_8\text{O}_7 \cdot \text{H}_2\text{O}$  as per the stoichiometric proportion of Co and Fe in CFO. The citric acid and metal nitrates were dissolved in deionized water according to their molar proportion. The pH of the solution was maintained to neutral value using liquid ammonia [7]. The solution was continuously stirred on magnetic stirrer at constant temperature of  $80^\circ\text{C}$  for uniform mixing and to obtain clear sol. The obtained sol was

then converted into the xerogel at  $120^\circ\text{C}$ . The continuous heating on magnetic stirrer leads to a self-propagating combustion reaction and after complete combustion the obtained CFO nanopowder was annealed at  $700^\circ\text{C}$  for 5 hours.

## RESULTS AND DISCUSSION

### 1. X ray Diffraction:

Crystal structure of the cobalt ferrite was examined using the X-ray diffraction (XRD) with Bruker D8 advanced diffractometer ( $\text{Cu K}\alpha$  radiation,  $\lambda = 1.54178 \text{ \AA}$ ). The XRD patterns obtained for  $\text{CoFe}_{2-x}\text{O}_4$  are shown in Figure 1. XRD pattern of CFO exhibits all the characteristic reflections with the most intense (311) peak. The XRD data confirms the formation of CFO matrix (JCPDS cards:22-1086) with single phase cubic spinel structure (space group  $\text{Fd}\bar{3}\text{m}$  (227)) without any trace of impurity. The lattice constant obtained from XRD is  $8.39 \text{ \AA}$ . The crystallite size ( $D$ ) of CFO samples was calculated using the well-known Scherrer formula [8]:

$$D = \frac{K\lambda}{\beta \cos\theta}$$

where  $K$  is related to crystallite shape, normally taken as 0.9,  $\lambda$  is the wavelength of X-ray in nanometer (nm),  $\beta$  is the full width at half maximum (in radians) of the diffraction peak. The result shows the decrease in crystallite size, 40 nm for the synthesized CFO nanoparticles.

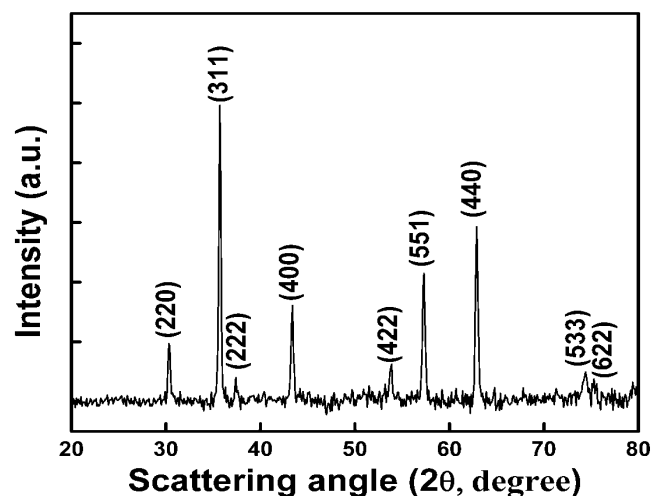


Figure 1. XRD pattern of Cobalt ferrite nanoparticles

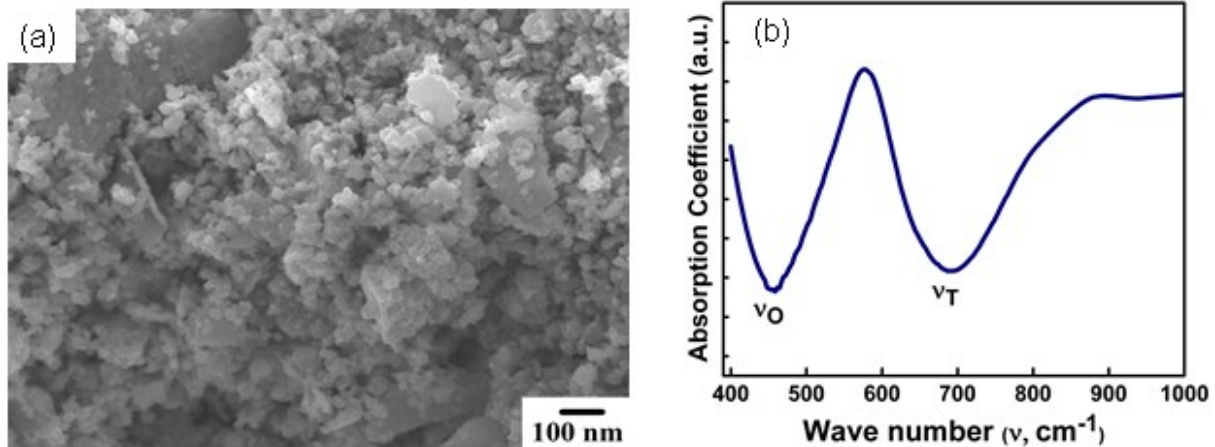


Figure 2 (a) FE-SEM image and (b) FT-IR Spectrum of Cobalt Ferrite nanoparticles

## 2. Surface Morphology:

The morphology and particle size of the synthesized cobalt ferrite nanoparticles by the sol gel auto combustion methods are studied using field emission scanning electron microscopy (FESEM). The instrument utilized to observe the microstructure was JEOL-JSM-6360. The FE-SEM image as shown in Figure 2(a), authenticates the spherical surface morphology for CFO nanoparticles. The average particle size obtained from FESEM image is of 42 nm. The agglomeration of magnetic nanoparticles may leads to the some large lumps as seen in FESEM photograph.

## 3. IR analysis:

The information on the chemical changes taking place during the synthesis can be obtained by infrared absorption spectra analysis. The IR spectra of annealed CFO nanoparticles at 700 °C are shown in Figure 2(b). The broadening of absorption peaks in IR spectrum authenticate the nanosized grains [9]. In ferrites, the metal ions are situated in two different sub lattices designated as tetrahedral (A-site) and octahedral (B-site) according to the geometrical configuration of the oxygen nearest neighbors. Waldron have attributed the absorption band around 700 cm<sup>-1</sup> to stretching vibrations of tetrahedral groups (v<sub>A</sub>) and around 400 cm<sup>-1</sup> to the octahedral group (v<sub>B</sub>) [10]. In the present study, the IR spectra shows two main absorption bands (v<sub>1</sub>) and (v<sub>2</sub>) that were observed at nearly 694 cm<sup>-1</sup> and 458 cm<sup>-1</sup> which corresponds to the stretching vibration of the tetrahedral and octahedral sites of spinel lattice, respectively [10]. The position and intensities of v<sub>1</sub> and v<sub>2</sub> vary slightly due to the difference in

the (Fe<sup>3+</sup> - O<sup>2-</sup>) distances for the tetrahedral and octahedral sites. In the present case, it is observed that due to Co<sup>2+</sup> content, v<sub>1</sub> shifts to lower frequency side while v<sub>2</sub> shifts to the higher frequency side, and this may be due to changes that occurred in the cation distribution of the spinel lattice. Here an increase of the population of Co<sup>2+</sup> (0.78 Å<sup>3</sup>) cations and decrease of Fe<sup>3+</sup> (0.64 Å<sup>3</sup>) cations at the A site contributes to the increase of ionic radii of the A site while a decrease of the population of Co<sup>2+</sup> cations at the B site contributes to the decrease of ionic radii of the B site. Furthermore, the change in the spectral position is expected because of the difference in the (Fe<sup>3+</sup>- O<sup>2-</sup>) distances for the octahedral and tetrahedral complexes. It was found that the (Fe<sup>3+</sup>- O<sup>2-</sup>) distance of the A site (0.189 nm) is smaller than that of B site (0.199 nm) [11]. As the vibrational frequency is proportional to force constant (K), the band shift of v<sub>1</sub> and v<sub>2</sub> to lower and higher frequency with Co<sup>2+</sup> occupancy indicates that the change in force constant. The calculated values of the force constant are 352 dyne/cm (K<sub>T</sub>) and 153 dyne/cm (K<sub>O</sub>) for A and B sites respectively. The following relation are utilized to calculate force constant [12].

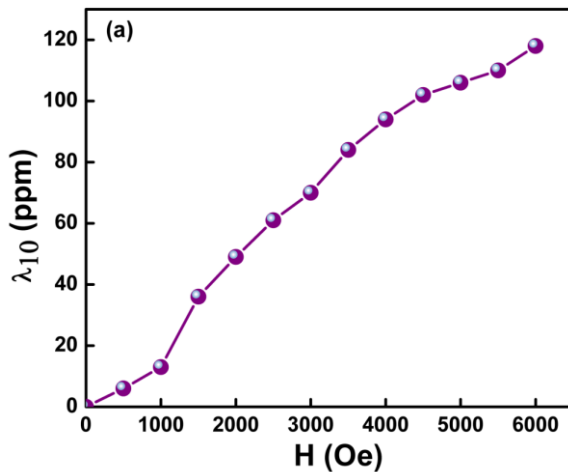
$$K = 4\pi^2c^2 v^2m;$$

where K is the force constant, c is Speed of light ~ 2.99 × 10<sup>8</sup> m/sec, v is the vibration frequency of the A and B sites, m is reduced mass for the Fe<sup>3+</sup> ions and the O<sup>2-</sup> ions (~2.065×10<sup>23</sup>gm/mol).

## 4. Magnetostrictive Properties:

Magnetostriction is measured at room temperature up to a maximum magnetic field strength of 6 kOe in

both parallel as well as the perpendicular directions to



the applied magnetic field. The magnetostriction

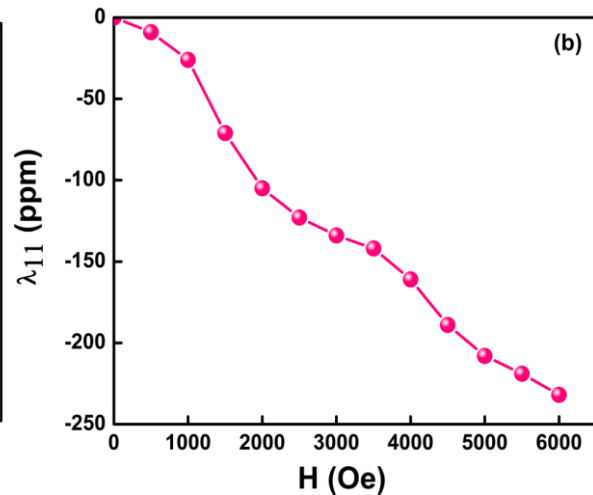


**Figure 3.** Magnetostriction as a function of magnetic field recorded in the (a) perpendicular direction ( $\lambda_{10}$ ) and (b) parallel direction ( $\lambda_{11}$ ) to the applied magnetic field.

curves recorded for cobalt ferrite prepared via modified sol gel auto combustion method are shown in Figure 3 (a) and 4(b), respectively. The highest magnetostriction is obtained for the sample synthesized by the auto combustion method and the lowest value is obtained for the sample synthesized by the ceramic method [13-14]. This may be due to the lower grain size [9, 13]. cobalt ferrite prepared by the combustion method shows an enhanced magnetostriction of 197 ppm at the lower value of applied magnetic field (6 kOe). The magnetostriction curves recorded in the perpendicular direction ( $\lambda_{\perp}$ ) for synthesized CFO also shows higher values than the reported values [14]. Thus, the presence of smaller and uniform sized grains seen in microstructure plays an important role in enhancing the magnetostrictive properties of cobalt ferrite for stress sensitivity.

### 5. Cation Distribution:

The cation distribution of the synthesized cobalt ferrite was obtained by using Mössbauer spectroscopy technique. The cation distribution is represented using the formula  $[\text{Co}_{1-x}\text{Fe}_x]_A[\text{Co}_x\text{Fe}_{2-x}]_B\text{O}_4$ , where  $x$  is the inversion parameter. Mössbauer spectra of the synthesized CFO nanoparticles shown in Figure 4.

The ratio of area under the absorption curve was considered for the determination of cation distribution of  $\text{Fe}^{3+}$  ions among the tetrahedral (A) and octahedral (B) interstitial sites. In ideal inverse spinel structure  $\text{Fe}^{3+}$  ions are equally distributed at A and B site of face

centre cubic oxygen lattice are filled by  $\text{Fe}^{3+}$  and  $\text{Co}^{2+}$  ions. However in real practice the degree of inversion is not complete in cobalt ferrite matrix [14-16]. This may be due to the heat treatment provided to the sample during synthesis affects the degree of inversion [13-16]. The obtained cation distribution is:  $[\text{Co}_{0.21}\text{Fe}_{0.79}]_{\text{tet}}[\text{Co}_{0.79}\text{Fe}_{1.21}]_{\text{oct}}\text{O}_4$ , shows that  $\text{Co}^{2+}$  ions are migrated towards tetrahedral site from the octahedral site. This may be due to the strong A-B super exchange lattice interaction [13-16].

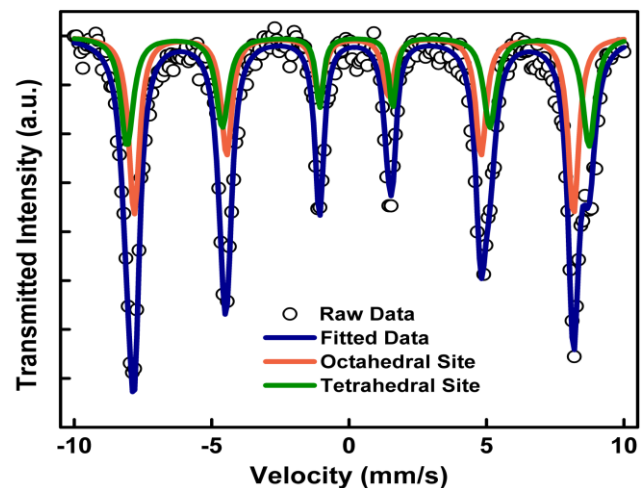


**Figure 4** Mössbauer spectrum of cobalt ferrite nanoparticles.

## CONCLUSION

Nanoparticles of  $\text{CoFe}_2\text{O}_4$  were successfully synthesized using sol-gel auto combustion method.

XRD analysis confirms the formation of cubic spinel structure without any impurity phases. XRD and FESEM results authenticate the nanometer regime of synthesized CFO. Magnetostrictive properties signify the use of sample in automotive sensing. IR spectroscopy and Mössbauer spectroscopy confirms the cation distribution of  $\text{Co}^{2+}$  ions among A and B site, hence authenticate the physical properties of the synthesized cobalt ferrite for possible spintronic applications.

**Conflicts of interest:** The authors stated that no conflicts of interest.

## REFERENCES

1. Limaye MV, Singh SB, Date SK, Kothari D, Reddy VR, Gupta A, Sathe V, Choudhary R and Kulkarni SK, *J. Phys. Chem. B*, 2009; 113, 9070-9076 (2009)
2. Prathapani S, Monaji VR, Jayaraman TV and Das D. *J. Appl. Phys.*, 2014; 116, 023908.
3. Kakade SG, Ma Y, Kolekar YD and Ramana CV, *J. Phys. Chem. C*, 2016; 120, 5682-5693.
4. Tiwari Dharmendra K, Behari J, Sen P, *World App.Sci. J.* 2008; 417.
5. Mazario E, Menéndez N, Herrasti P, Cañete M, Connord V and Carrey J, *J. Phys. Chem. C*, 2013; 117, 11405-11411.
6. Shinde SS, S Singh Meena, S. M. Yusuf, and K. Y. Rajpure, *J. Phys. Chem. C*, 2011; 115, 3731-3736.
7. Kakade SG, Kambale RC and Kolekar YD, AIP Conf. Proc., 2015; 1665, 130057.
8. Kulkarni SK. *Nanotechnology: Principles and Practices*, Springer Publication (2014).
9. Naik SR and Salker AV. *J. Mater. Chem.*, 2012; 22, 2740-2750.
10. Waldron RD. *Phys. Rev.*, 1955; 99, 1727.
11. Zaki HM, Dawoud HA. *Physica B*, 2010; 405, 4476.
12. Zhoua B, Zhanga Y, Liaoa C, Yana CH and Wangb SY. *J. Magn. Magn. Mater.*, 2004; 280:327.
13. Kakade SG, Kambale RC, Ramanna CV and Kolekar YD. *RSC Adv.*, 2016; 6, 33308-33317.
14. Bharati Kamala K, Ph. D. Thesis, I. I. T, Chennai, (2010).
15. Krieble K. *J. Appl. Phys.*, 2008; 103, 07E508.
16. Kharat SP, Darvade TC, Gaikwad SK, Baraskar BG, Kakade SG, Kambale RC and Kolekar YD. AIP Conference Pro., 1731, 130056, (2016)

© 2018 | Published by IRJSE

### Submit your manuscript to a IRJSE journal and benefit from:

- ✓ Convenient online submission
- ✓ Rigorous peer review
- ✓ Immediate publication on acceptance
- ✓ Open access: articles freely available online
- ✓ High visibility within the field

Email your next manuscript to IRJSE

: editorirjse@gmail.com